Volume 11
Number 31
21 August 2020
Pages 4953-5100

Polymer Chemistry

rsc.li/polymers

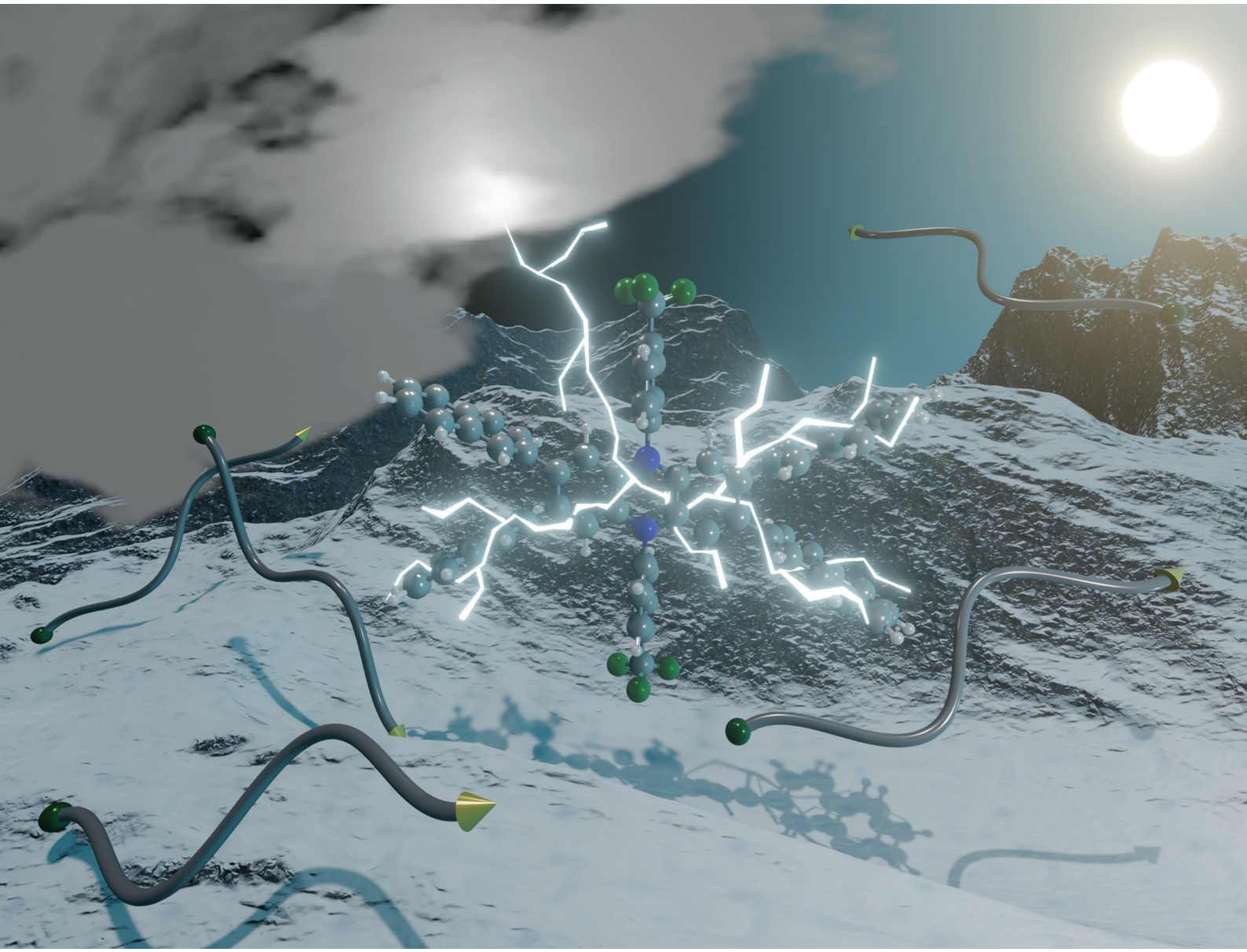

ISSN 1759-9962

ROYAL SOCIETY OF CHEMISTRY

PAPER
Garret M. Miyake *et al.*
Impacts of performing electrolysis during organocatalyzed atom transfer radical polymerization

Polymer Chemistry

ROYAL SOCIETY OF CHEMISTRY

PAPER

View Article Online
View Journal | View Issue

Cite this: *Polym. Chem.*, 2020, **11**, 4978

Impacts of performing electrolysis during organocatalyzed atom transfer radical polymerization†

Daniel A. Corbin, Blaine G. McCarthy and Garret M. Miyake *

An electrochemical variant of organocatalyzed atom transfer radical polymerization (O-ATRP) is developed and investigated. Inspired by electrochemically mediated atom transfer radical polymerization (eATRP), potentiostatic electrolysis is used to manipulate the catalyst's redox states in O-ATRP to understand whether deactivation in O-ATRP can be enhanced to improve polymerization control. During the course of this work, several possible side reactions are investigated, and the electrochemical apparatus is optimized to reduce side reactions at the counter electrode. This electrochemically modified O-ATRP method (eO-ATRP) is then studied at different applied potentials, under different irradiation conditions, and with two photoredox catalysts to understand the impact of electrolysis on polymerization control. Ultimately, although electrolysis was successfully used to improve polymerization control in O-ATRP, some additional challenges have been identified. Several key questions are postulated to guide future work in this area.

Received 30th April 2020,
Accepted 25th June 2020

DOI: 10.1039/d0py00643b

rsc.li/polymers

Introduction

First reported in 2014, organocatalyzed atom transfer radical polymerization (O-ATRP) is a controlled radical polymerization method employing organic photoredox catalysts (PCs) for the production of polymers with targeted molecular weights and architectures.[1,2] The proposed mechanism of O-ATRP proceeds through absorption of light by a PC to access an excited state (PC*). This excited state then reduces the alkyl-halide(bromide) bond of an initiator or polymer chain-end to generate the PC radical cation ($PC^{\bullet+}$), Br^-, and 'active' radicals capable of polymerization propagation with vinyl monomers (Fig. 1). Importantly, the $PC^{\bullet+}$ that forms mediates deactivation in O-ATRP, during which bromide is reinstalled on the chain-end of a polymer to generate a 'dormant' species and the ground state PC.[1–4] It has been proposed that deactivation in O-ATRP could proceed through a termolecular reaction, in which $PC^{\bullet+}$, Br^-, and the radical chain-end react simultaneously to form the dormant polymer and ground state PC.[5] While computational results support that this termolecular reaction is thermodynamically feasible, our working hypothesis is that deactivation proceeds through a bimolecular reaction, in which $PC^{\bullet+}$ and Br^- preassociate to form the $PC^{\bullet+}Br^-$ ion pair that then reacts with the propagating radical. Regardless of the exact mechanism of this process, the effect is the same: deactivation reduces the concentration of radicals in solution and thereby suppresses radical-based termination reactions, which would otherwise hinder control over polymer structure.[6–10]

Since the inception of this method, much work has focused on expanding the utility of O-ATRP through various approaches. Some strategies have focused on the development of new photoredox catalysts[3,4,11–17] as a means to access the polymerization of new monomers, such as acrylonitrile[11] and acrylates.[17] Alternatively, other advancements have come through the application of O-ATRP for the synthesis of materials with advanced architectures[18,19] and applications,[20,21] while some investigations have focused on understanding the mechanism of O-ATRP[5,22] and the structure–property relationships of the PCs[3,4,15,23–25] employed therein. Despite these advancements, the monomer scope of O-ATRP and its ability to produce polymers of high molecular weight[26–31] remains limited, especially in comparison to metal catalyzed ATRP.[32]

To overcome these limitations and further advance the O-ATRP method, more detailed investigation of the deactivation mechanism and methods to control this process are desirable. In some sense, modulation of deactivation has been attempted through the development of new PCs with more oxidizing radical cations,[17] which might mediate a faster deactivation process than less oxidizing radical cations. However, we envisioned a more direct approach to study the deactivation

Department of Chemistry, Colorado State University, Fort Collins, Colorado 80523-1872, USA. E-mail: garret.miyake@colostate.edu

†Electronic supplementary information (ESI) available. See DOI: 10.1039/d0py00643b

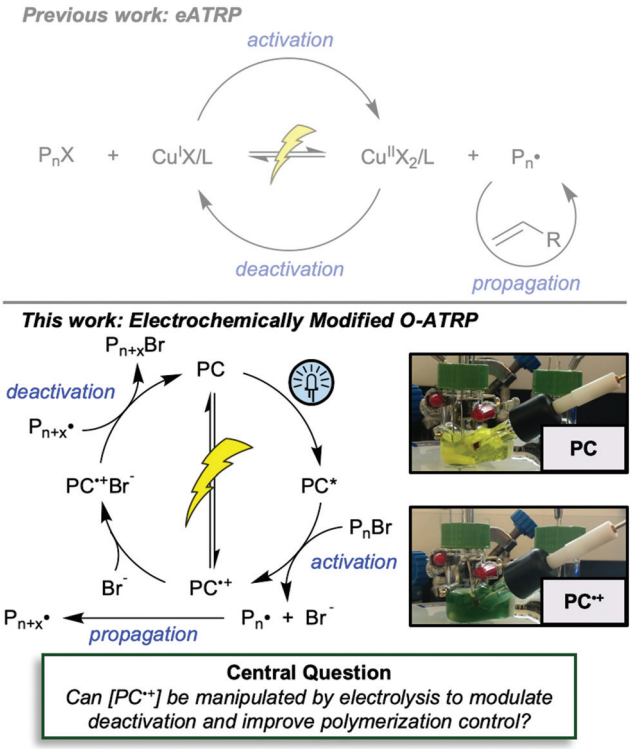

Fig. 1 Previous work demonstrated the ability to mediate ATRP using electrochemistry (top). In this work (bottom), we ask whether this principle can be applied to O-ATRP to control the concentration of $PC^{\bullet+}$ and thereby control deactivation in this polymerization method. Figure inset (bottom right) demonstrates the conversion of PC to $PC^{\bullet+}$ using potentiostatic bulk electrolysis.

process would be to manipulate the concentration of deactivator present rather than the oxidation potential of the species. To achieve this effect, we drew inspiration from electrochemically mediated ATRP (eATRP, Fig. 1), wherein electrochemistry has been used to control activator and deactivator concentrations in metal catalyzed ATRP and mediate controlled polymerizations under a range of different conditions.[33–37] Analogously, one can envision manipulating the concentration of $PC^{\bullet+}$ in solution by potentiostatic electrolysis of the PC (Fig. 1, inset) according to the Nernst equation (eqn (1)). By performing this process to generate a higher $[PC^{\bullet+}]$ *in situ*, it might be possible to increase the rate of deactivation to afford enhanced polymerization control in challenging systems. As such, this work probes whether electrolysis of the PC can be used during O-ATRP to increase the $[PC^{\bullet+}]$ to improve deactivation, as well as the impact of performing electrolysis on the polymerization solution.

$$\frac{[PC^{\bullet+}]}{PC} = e^{\frac{F(E_{app}-E_{1/2})}{RT}} \quad (1)$$

The Nernst equation relates the applied electrochemical potential (E_{app}) to the ratio of PC to $PC^{\bullet+}$ at the electrode surface where F is Faraday's constant [C mol^{-1}], E_{app} is the applied electrochemical potential [V], $E_{1/2} \sim E^{\circ}(PC^{\bullet+}/PC)$ determined by cyclic voltammetry [V], R is the ideal gas constant [J mol^{-1} K^{-1}], and T is the absolute temperature [K]. Using rapid stirring, this ratio can be manipulated in the bulk solution.

Results and discussion

Initial conditions and polymerization results

The central hypothesis of this work is that by applying an appropriate electrochemical potential (E_{app}), the concentration of $PC^{\bullet+}$ (the deactivator) in O-ATRP can be manipulated to improve polymerization control. Polymerization control in this work was determined by four criteria: (1) linear pseudo-first order kinetics of monomer conversion, (2) linear and increasing molecular weight (M_n) as a function of monomer conversion, (3) decreasing and low dispersity ($Đ$ < 1.5) during the course of polymerization, and (4) achieving initiator efficiency near 100% ($I^* = M_{n,\,theo}/M_{n,\,exp}$).

To investigate the effects of increasing the concentration of $PC^{\bullet+}$ in O-ATRP using electrolysis, a degree of polymerization (DP) of 200 was targeted since previous reports at this DP exhibited only moderate control relative to lower targeted DPs.[3,4,16] Moreover, to minimize the possibility of introducing redox side reactions, dihydrophenazine PCs were employed, since this family of PCs would require application of the least oxidizing potential to achieve a higher concentration of $PC^{\bullet+}$ relative to other PC families. However, within the dihydrophenazine family, radical addition to the phenazine core has been proposed as a possible side reaction leading to poor initiator efficiency in O-ATRP. As such, PC **1** was chosen because the core-positions of this PC are blocked by naphthyl substituents (Fig. 2), reducing the risk of this PC reacting undesirably with radicals in solution.[16] With this PC chosen, all other polymerization conditions (Fig. 2) were selected based on published conditions for O-ATRP using PC **1**.[16]

For the supporting electrolyte (SE), a 0.1 M mixture of tetra-*n*-butylammonium hexafluorophosphate (Bu_4NPF_6, 94%) and tetra-*n*-butylammonium bromide (Bu_4NBr, 6%) was initially chosen based on conditions reported for eATRP[33] and altered later. A lower E_{app} was used relative to eATRP [$E_{app} = E_{1/2} -$ 120 mV *vs.* $E_{app} \sim E_{1/2}(Cu^{II}/Cu^{I})$]. In eATRP, both the concentrations of Cu^{I} and Cu^{II} can be manipulated by electrolysis, directly impacting both activation and deactivation. However, in O-ATRP activation is mediated by PC* (Fig. 1), the concentration of which is likely dependent on the intensity of the light source. In fact, based on published data[38] for common PCs in O-ATRP, estimates indicate that only up to about 1% of the PC exists as PC* under steady state conditions (see Estimation of excited state PC concentration in ESI†). As such, electrolysis conditions were chosen to produce roughly 1% $PC^{\bullet+}$ based on eqn (1). Finally, to prevent side reactions from occurring at the counter electrode, a U-cell was chosen with a very-fine glass frit separating the counter electrode from the polymerization solution (see Experimental equipment in ESI†).

To evaluate the impact of electrolysis on polymerization control, eO-ATRP was conducted in the presence of an oxidiz-

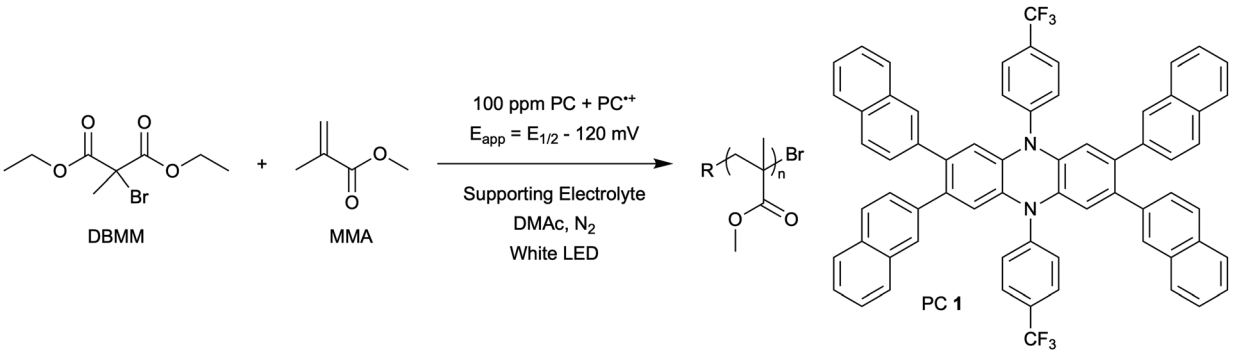

Fig. 2 General scheme for the eO-ATRP of MMA using DBMM as the initiator and 100 ppm of PC **1**.

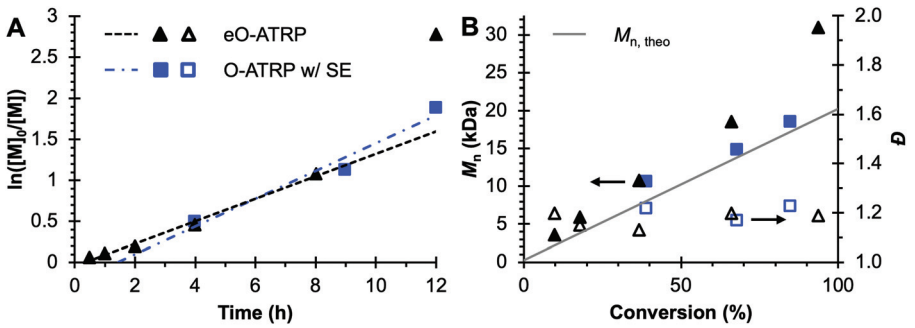

Fig. 3 Plot of the natural logarithm of monomer (M) consumption over time (A). Molecular weight (filled markers) and $Đ$ (hollow markers) evolution (B) for eO-ATRP (black triangles) and O-ATRP with supporting electrolyte (blue squares). Conditions: [MMA] : [DBMM] : [**1**] = [1000] : [5] : [0.1], 2 mL MMA, 2 mL DMAc, SE = 0.094 M Bu_4NPF_6 and 0.006 M Bu_4NBr. Reactions performed in a U-cell and irradiated with a high-power white LED (see Experimental equipment in ESI†). For eO-ATRP, working electrode = glassy carbon, counter electrode = Pt wire, reference electrode = Ag wire quasi-reference electrode, and $E_{app} = E_{1/2} - 120$ mV.

ing applied potential ($E_{app} = E_{1/2} - 120$ mV) (Fig. 3). It was hypothesized that these eO-ATRP conditions would lead to a slower overall rate of polymerization and the synthesis of PMMA with lower $Đ$, yet neither effect was observed. The observed rate constants of the polymerizations (O-ATRP = 0.17 h^{-1}, eO-ATRP = 0.14 h^{-1}) and $Đ$ of the PMMA synthesized ($Đ$ = 1.23 for O-ATRP, $Đ$ = 1.19 for eO-ATRP) were similar. Unexpectedly, eO-ATRP exhibited some loss of control, with I^* values deviating significantly from 100%, especially at higher monomer conversions (I^* = 72% at 66% conversion and I^* = 61% at 94% conversion).

Hypotheses for poor control

In total, nine hypotheses to explain the observed data were formulated. While all nine hypotheses are stated below, hypotheses 1–8 are also depicted schematically in Table 1.

1. Due to the highly reducing nature of PC* [$E°(\mathbf{1}^{\bullet+}/\mathbf{1}^*) \sim -1.8$ V *vs.* SCE],[16] tetra-*n*-butylammonium cation (Bu_4N^+) is reduced to form a reactive species that hinders polymerization control. This process likely occurs through formation of $Bu_4N^{\bullet}$, which rapidly decomposes to tributylamine and butyl radical.[39] The amine may act as an electron donor to quench $PC^{\bullet+}$, leading to poor deactivation. Further, butyl radical formation could lead to unwanted initiation and termination events in the polymerization.

2. MMA is oxidized at the surface of the working electrode to generate a reactive species, which either reacts with the PC or interrupts the polymerization.

3. DBMM is oxidized at the surface of the working electrode to generate a reactive species, which either reacts with the PC or interrupts the polymerization. Consumption of the initiator through this side reaction would also lower I^*.

4. Bromide ion, either from the supporting electrolyte or the activation of an alkyl-bromide bond, is oxidized at the working electrode, generating a bromine radical capable of initiating polymer chains.

5. Photoexcitation of $PC^{\bullet+}$ generates a strongly oxidizing excited-state species, which oxidizes DMAc to generate a reactive radical capable of performing initiation and termination reactions.

6. Photoexcited $PC^{\bullet+}$ oxidizes the radical chain-end of a propagating polymer, generating a reactive carbocation that rapidly and irreversibly terminates under O-ATRP conditions.

7. Photoexcited $PC^{\bullet+}$ oxidizes Br^-, either from the supporting electrolyte or from the activation of an alkyl-bromide bond, generating a bromine radical capable of initiating new polymer chains.

8. Hexafluorophosphate from the supporting electrolyte competitively ion-pairs with $PC^{\bullet+}$ to form $PC^{\bullet+}PF_6^-$, leading to poor polymerization control. If this process occurs to a signifi-

Table 1 Schematic representations of hypotheses 1–8 for the investigation of potential side reactions that can occur during eO-ATRP

Hypothesis	Scheme	Key data
1	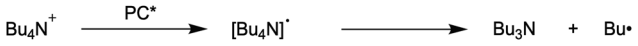	Table 2, entry 1; Fig. S34†
2	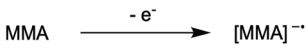	Fig. S35†
3	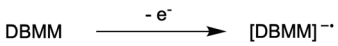	Fig. S36†
4	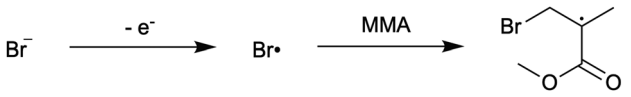	Table 2, entry 2; Fig. S37†
5	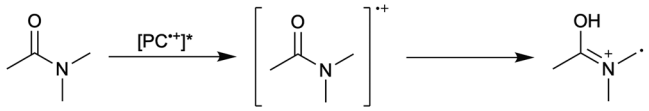	Hypothesis not disproved
6	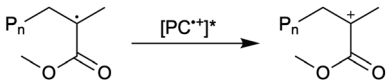	Kinetically unlikely (see text)
7	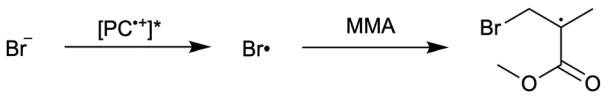	Hypothesis not disproved (see text)
8		Table 2, entry 3; Fig. S39†

cant extent, it would limit the formation of $PC^{\bullet+}Br^{-}$ and thereby reduce the rate of deactivation.

9. Under current conditions, the counter electrode is insufficiently separated from the polymerization. As such, control is lost either as the PC and $PC^{\bullet+}$ diffuse to the counter electrode and undergo degradation, or as reactive species produced at the counter electrode diffuse into the polymerization and cause side reactions.

With these hypotheses in hand, experiments were then devised to test and support or disprove each one. For example, in hypothesis 1, it is proposed that the reduction of Bu_4N^+ (hypothesis 1) could be responsible for side reactivity in eO-ATRP leading to poor control. If this hypothesis is true, changing the supporting electrolyte to $LiPF_6$ (Table 2, entry 1; also see ESI†) should eliminate reduction of the cation and thereby improve the polymerization outcome, as **1*** should not be able to reduce Li^+. Of course, this experiment is based on the assumption that no other significant side reactivity would occur with $LiPF_6$, but this assumption is supported by later experiments with this supporting electrolyte (*vide infra*). However, no improvement in polymerization control was observed in this experiment ($Đ$ = 2.08, I^* = 82%), disproving hypothesis 1.

Table 2 Polymerization results related to tests of hypotheses 1, 4, and 8. For full experimental details, please see the Control experiments section of the ESI†

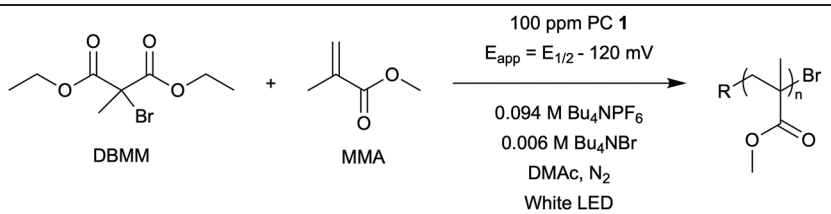

Entry	Deviation from scheme	Hypothesis tested	Conv. (%)	$M_{n,\,theo}$ (kDa)	$M_{n,\,GPC}$ (kDa)	$Đ^a$	$I^{*\,b}$ (%)
1	SE = 0.1 M $LiPF_6$	1	77	15.7	19.2	2.08	82
2	No PC or light	4	0	—	—	—	—
3	No electrolysis, SE = 0.1 M $LIPF_6$	8	68	13.8	12.1	1.17	114

[a] Calculated by M_w/M_n. [b] Calculated by $M_{n,\,theo}/M_{n,\,GPC}$.

To test hypotheses 2–4, cyclic voltammetry (CV) was performed to examine the redox behavior of each component of the polymerization solution. Since the CV of **1** in DMAc with 0.1 M Bu_4NPF_6 has previously been reported elsewhere,[16] the redox stability of the solvent and this supporting electrolyte were not examined. To test the redox stability of MMA (hypothesis 2), CV was used to examine a mixture of MMA and DMAc in a ratio corresponding to that used in eO-ATRP (Fig. S35†). No current response was observed in the relevant potential range (−0.1–0.1 V *vs.* $Ag/AgNO_3$), disproving hypothesis 2. Next, DBMM was added to the solution and its redox stability (hypothesis 3) was examined by CV, which revealed only a reduction peak around −1.2 V *vs.* $Ag/AgNO_3$ (Fig. S36†). Since no response was observed in the range relevant to eO-ATRP, these data disprove hypothesis 3.

A similar experiment was performed to test for Br^- oxidation at the working electrode (hypothesis 4), where CV was used to examine a solution of 0.1 M Bu_4NPF_6 (94%) and Bu_4NBr (6%) in MMA and DMAc. This time, an irreversible oxidation followed by a quasi-reversible redox couple was observed (Fig. S37†), presumably corresponding to Br^- oxidation to form Br_3^-, followed by oxidation of Br_3^- to form Br_2.[39–43] However, no current response was seen in the appropriate potential range for eO-ATRP, indicating this redox reaction is unlikely to interfere in these polymerizations. Further evidence to disprove this hypothesis was found in a control reaction excluding **1** and light (see Control experiments section in ESI†). If Br^- oxidation at the working electrode could lead to unwanted polymerization of MMA, it should be observable under these conditions. However, proton NMR analysis of the reaction solution after 24 h of electrolysis showed no polymer formation (Table 2, entry 2), disproving hypothesis 4.

Since no evidence could be found for deleterious side reactivity at the working electrode, hypotheses 5–7 for possible side reactions involving photoexcited $PC^{\bullet+}$ were considered next. Each hypothesis is based on the concept that $PC^{\bullet+}$ might be able to access a strongly oxidizing excited state by absorption of visible light. In turn, photoexcitation of this species might lead to the oxidation of DMAc (hypothesis 5), the radical chain-end of a propagating polymer (hypothesis 6), or Br^- (hypothesis 7). Currently, no evidence exists to disprove the oxidation of DMAc by this species (hypothesis 5), so this hypothesis will be revisited later in the text (*vide infra*).

With regard to the oxidation of the chain-end radical (hypotheses 6), the ground state of $PC^{\bullet+}$ is not sufficiently oxidizing to directly cause this side reaction, necessitating photoexcitation to make the oxidation thermodynamically feasible. However, it seems unlikely that this reaction would occur to a significant extent considering that the components of this reaction should both be in low concentrations. Due to deactivation in O-ATRP, the formation of chain-end radicals should be suppressed to prevent radical-coupling reactions. In addition, it seems unlikely that the concentration of photoexcited $PC^{\bullet+}$ would be sufficient to react with this species to a significant degree, since the lifetimes of photoexcited species are generally quite short (10^{-9}–10^{-6} s) and most of the $PC^{\bullet+}$ should exist in the ground state. Of course, this argument does not necessarily mean that this side reaction does not take place in eO-ATRP. However, based on these kinetics considerations as well as experiments related to hypothesis 9 (*vide infra*), this side reaction does not appear sufficient to explain the current issues observed in eO-ATRP.

With regard to the oxidation of Br^- by photoexcited $PC^{\bullet+}$ (hypothesis 7), while a bimolecular reaction between Br^- and photoexcited $PC^{\bullet+}$ could be considered unlikely based on the same kinetic argument that is presented above (at least in the absence of a bromide-containing supporting electrolyte), it is also possible that $PC^{\bullet+}$ and Br^- could associate prior to photoexcitation. If photoexcitation of the $PC^{\bullet+}Br^-$ ion pair occurred, the oxidation of Br^- would be more feasible given the close proximity of these species, which would reduce the necessity for a long-lived $PC^{\bullet+}$ excited state. Currently, no evidence exists to rule out the photoexcitation of $PC^{\bullet+}Br^-$. However, to our knowledge, no evidence for this side reaction in O-ATRP has yet been found, as the prevalence of this reaction would hinder the production of well-defined polymers by O-ATRP. Further, since an improvement in polymerization control was observed in experiments related to hypothesis 9 (*vide infra*), where this side reaction would have still been present, this reaction does not appear to be a significant contributor to poor control in eO-ATRP.

Another possibility that was considered is competitive ion pairing between $PC^{\bullet+}$ and either Br^- or PF_6^- (hypothesis 8). Depending on the relative strengths of ion pairing in $PC^{\bullet+}Br^-$ and $PC^{\bullet+}PF_6^-$, it is possible that the formation of $PC^{\bullet+}PF_6^-$ might prevent the formation of $PC^{\bullet+}Br^-$ and thereby lower the rate of deactivation. To test this hypothesis, O-ATRP was carried out in the presence of 0.1 M $LiPF_6$ (Table 2, entry 3; also see Fig. S39†), yielding PMMA with low $Đ$ ($Đ$ = 1.17) and good molecular weight control (I^* = 114%). While this experiment does not indicate whether competitive ion pairing is present in eO-ATRP, it does suggest this interaction does not limit polymerization control, disproving hypothesis 8.

Therefore, the remaining hypotheses that were considered are the oxidation of DMAc by photoexcited $PC^{\bullet+}$ (hypothesis 5) and insufficient separation of the counter electrode from the reaction solution (hypothesis 9). To test hypothesis 9, a new apparatus (Fig. 4) was employed featuring a vycor-glass frit (pore size ∼ 4 nm (ref. 44)) to separate the counter electrode instead of the previously used U-cells with very-fine glass frits (pore size ∼ 2 μm (ref. 45)). Excitingly, eO-ATRP with 0.1 M $LiPF_6$ as the supporting electrolyte exhibited excellent control (Table 3, entry 4: $Đ$ = 1.17, I^* = 110%), with I^* near 100% and $Đ$ below 1.2 for nearly the entire polymerization (Fig. 5). Further, while this experiment does not directly test hypothesis 5 for DMAc oxidation by photoexcited $PC^{\bullet+}$, it does suggest this side reaction is less significant, as its effects should have been observable even under these new experimental conditions. Based on this result and complying with Ockham's razor,[46] hypothesis 9 appears to be the simplest explanation for why eO-ATRP initially showed limited improvement over O-ATRP under similar conditions. As such, all future experi-

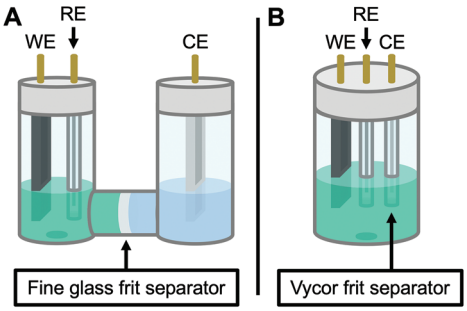

Fig. 4 Diagram of the apparatus used in this work. Originally, a modified U-cell was employed to separate the working and counter electrode compartments (A). When this separator was found to be ineffective on the time scale of eO-ATRP, a new apparatus was developed using a 5-neck electrochemical flask (see Experimental equipment in ESI†) and vycor frit separators to isolate the counter electrode (B). WE = working electrode, RE = reference electrode, and CE = counter electrode.

Table 3 Results for the eO-ATRP of MMA using the electrochemical cell in Fig. 4B

Entry	Control[a]	Conv. (%)	$M_{n,\,theo}$ (kDa)	$M_{n,\,GPC}$ (kDa)	$Đ^b$	$I^{*\,c}$ (%)
4	None	69	14.0	12.8	1.17	110
5	No electrolysis	52	10.7	8.47	1.33	127
6	No SE	68	13.8	11.0	1.27	126
7	No PC	7	1.56	52.7	2.23	3.0
8	No initiator	63	—	239	1.94	—
9	No light	0	—	—	—	—
10	No PC or light	0	—	—	—	—

[a] General conditions unless otherwise stated: [MMA] : [DBMM] : [**1**] = [1000] : [5] : [0.1], 2 mL MMA, 2 mL DMAc, SE = 0.1 M $LiPF_6$. Reactions performed in a 5-neck pear flask and irradiated with an 80 mm × 40 mm white LED well (9 LED segments, see Experimental equipment in ESI†). Where applicable, working electrode = glassy carbon, counter electrode = Pt wire, reference electrode = $Ag/AgNO_3$, and $E_{app} = E_{1/2} - 120$ mV. [b] Calculated by M_w/M_n. [c] Calculated by $M_{n,\,theo}/M_{n,\,GPC}$.

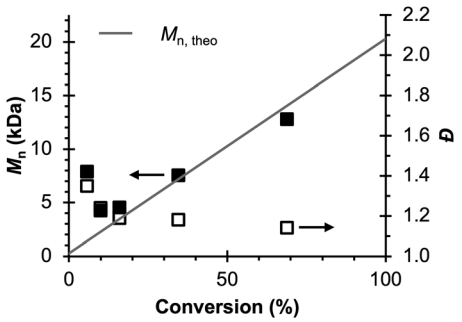

Fig. 5 Evolution of molecular weight (filled squares) and $Đ$ (hollow squares) for eO-ATRP using a vycor-glass frit to separate the counter electrode from the polymerization solution. Conditions: [MMA] : [DBMM] : [**1**] = [1000] : [5] : [0.1], 2 mL MMA, 2 mL DMAc, SE = 0.1 M $LiPF_6$. Reaction performed in a 5-neck pear flask and irradiated with an 80 mm × 40 mm white LED well (9 LED segments, see Experimental Equipment in ESI†). Working electrode = glassy carbon, counter electrode = Pt wire, reference electrode = $Ag/AgNO_3$, and $E_{app} = E_{1/2} - 120$ mV.

ments were performed with this new apparatus using vycor-glass separators for the counter and reference electrodes.

Impact of reaction parameters on control

To evaluate how each reaction component contributes to eO-ATRP, control polymerizations were performed (Table 3). In the absence of electrolysis (entry 5) or supporting electrolyte (entry 6), a controlled polymerization was still observed, but $Đ$ and I^* both rose ($Đ$ = 1.33 and 1.27, I^* = 127% and 126%, respectively) relative to eO-ATRP ($Đ$ = 1.17, I^* = 110%). These data demonstrate that improvement in polymerization control can be obtained by the application of an electrochemical potential. Reactions performed in the absence of PC (entry 7) or initiator (entry 8) exhibited characteristics of a free radical polymerization ($Đ$ = 2.23 and 1.94, respectively), whereas reactions in the dark – with or without PC, entries 9 and 10, respectively – showed no conversion by ^1H NMR after 24 hours.

Further influences on polymerization control were studied by variation of the light source, application of a more oxidizing electrochemical potential, and use of a different PC (see Supplemental polymerization data in ESI†). Similar to previous O-ATRP systems,[47] it was found that intensity of the light source had a significant impact on polymerization control. Lowering the intensity of the light caused a decrease in polymerization control, as observed by a gradual increase in $Đ$ and deviation of I^* from 100% (Fig. S43 and S44†). Interestingly, while a small increase in light intensity afforded similar control (Fig. S45†), large increases in light intensity from use of high-power LEDs resulted in a decrease in control (Fig. S48 and S49†). When a more oxidizing electrochemical potential was applied to this system ($E_{app} = E_{1/2} - 60$ mV) to compensate for a possible increase in the rate of activation, further loss of control was observed (Fig. S50†). While this result is consistent with the possibility of a side reaction stemming from photoexcitation of $PC^{\bullet+}$, further investigation of this possible reactivity is necessary. Finally, eO-ATRP was attempted with 3,7-di(4-biphenyl)-1-naphthyl-10-phenoxazine (**2**) as the PC. However, no improvement in polymerization control was observed, as electrolysis led to a significant increase in $Đ$ and complete loss of molecular weight control (Fig. S52 and S53†).

Conclusion

In summary, through a number of control experiments, we have investigated the impact of performing electrolysis during O-ATRP to manipulate the concentration of deactivator in solution. Using cyclic voltammetry, several background reactions at the working electrode were evaluated and ruled out. The formation of bromine radical at the working electrode to initiate undesired polymerizations was further probed through a control polymerization, although this reaction did not appear operative under the conditions used in this work. Further, the impact of competitive ion pairing between the PC radical

cation and PF_6^- from the supporting electrolyte was studied but found to be insignificant under these conditions. While the possibility of side reactivity originating from photoexcitation of the PC radical cation was also proposed, ultimately it was discovered that optimization of the electrochemical apparatus to prevent side reactions at the counter electrode was most important for establishing a controlled polymerization.

Although some improvement in polymerization control was observed in eO-ATRP relative to O-ATRP, this work has revealed the complexity of performing electrolysis during O-ATRP. Based on these results, several questions arise that are the focus of our ongoing work and that we believe will further improve the results of eO-ATRP. These questions include:

1. What is the effect of the supporting electrolyte on PC redox and photophysical properties?

2. Is the PF_6^- anion truly inert, or does competitive ion-pairing occur to any degree that might impact polymerization control?

3. If competitive ion-pairing occurs, is this effect more prominent for certain PCs or PC families than others?

4. Are there any side reactions through which $PC^{\bullet+}$ is consumed during O-ATRP, such that increasing the concentration of $PC^{\bullet+}$ in eO-ATRP increases the occurrence of these degradation pathways?

5. Is $PC^{\bullet+}Br^-$ truly the deactivator in O-ATRP, or is another species responsible for this process?

Conflicts of interest

The authors declare no competing financial interests.

Acknowledgements

The authors are grateful for support provided by Colorado State University. Research reported in this publication was also supported by the National Institute of General Medical Sciences (Award R35GM119702) of the National Institutes of Health. The content is solely the responsibility of the authors and does not necessarily represent the official views of the National Institutes of Health. B. G. M. acknowledges support from the NSF GRFP. D. A. C. would also like to thank Dr Scott Folkman for helpful discussions on electrochemistry, as well as Max Kudisch and Tara Mensch for assistance with the design and assembly of 3D printed photoreactors used in this work.

References

1 G. M. Miyake and J. C. Theriot, *Macromolecules*, 2014, **47**, 8255–8261.
2 N. J. Treat, H. Sprafke, J. W. Kramer, P. G. Clark, B. E. Barton, J. R. de Alaniz, B. P. Fors and C. J. Hawker, *J. Am. Chem. Soc.*, 2014, **136**, 16096–16101.
3 J. C. Theriot, C. H. Lim, H. Yang, M. D. Ryan, C. B. Musgrave and G. M. Miyake, *Science*, 2016, **352**, 1082–1086.
4 R. M. Pearson, C. H. Lim, B. G. McCarthy, C. B. Musgrave and G. M. Miyake, *J. Am. Chem. Soc.*, 2016, **138**, 11399–11407.
5 X. C. Pan, C. Fang, M. Fantin, N. Malhotra, W. Y. So, L. A. Peteanu, A. A. Isse, A. Gennaro, P. Liu and K. Matyjaszewskit, *J. Am. Chem. Soc.*, 2016, **138**, 2411–2425.
6 J. C. Theriot, B. G. McCarthy, C. H. Lim and G. M. Miyake, *Macromol. Rapid Commun.*, 2017, **38**, 1700040.
7 E. H. Discekici, A. Anastasaki, J. R. de Alaniz and C. J. Hawker, *Macromolecules*, 2018, **51**, 7421–7434.
8 G. Yilmaz and Y. Yagci, *Polym. Chem.*, 2018, **9**, 1757–1762.
9 N. Corrigan, S. Shanmugam, J. T. Xu and C. Boyer, *Chem. Soc. Rev.*, 2016, **45**, 6165–6212.
10 M. Chen, M. J. Zhong and J. A. Johnson, *Chem. Rev.*, 2016, **116**, 10167–10211.
11 X. C. Pan, M. Lamson, J. J. Yan and K. Matyjaszewski, *ACS Macro Lett.*, 2015, **4**, 192–196.
12 S. Dadashi-Silab, X. C. Pan and K. Matyjaszewski, *Chem. – Eur. J.*, 2017, **23**, 5972–5977.
13 M. D. Ryan, J. C. Theriot, C. H. Lim, H. S. Yang, A. G. Lockwood, N. G. Garrison, S. R. Lincoln, C. B. Musgrave and G. M. Miyake, *J. Polym. Sci., Part A: Polym. Chem.*, 2017, **55**, 3017–3027.
14 V. K. Singh, C. Yu, S. Badgujar, Y. Kim, Y. Kwon, D. Kim, J. Lee, T. Akhter, G. Thangavel, L. S. Park, P. C. Nandajan, R. Wannemacher, B. Milian-Medina, L. Luer, K. S. Kim, J. Gierschner and M. S. Kwon, *Nat. Catal.*, 2018, **1**, 794–804.
15 B. G. McCarthy, R. M. Pearson, C. H. Lim, S. M. Sartor, N. H. Damrauer and G. M. Miyake, *J. Am. Chem. Soc.*, 2018, **140**, 5088–5101.
16 J. P. Cole, C. R. Federico, C. H. Lim and G. M. Miyake, *Macromolecules*, 2019, **52**, 747–754.
17 B. L. Buss, C. H. Lim and G. M. Miyake, *Angew. Chem.*, 2020, **59**, 3209.
18 B. L. Buss, L. R. Beck and G. M. Miyake, *Polym. Chem.*, 2018, **9**, 1658–1665.
19 Y. C. Zhao, H. H. Gong, K. M. Jiang, S. J. Yan, J. Lin and M. Chen, *Macromolecules*, 2018, **51**, 938–946.
20 E. H. Discekici, C. W. Pester, N. J. Treat, I. Lawrence, K. M. Mattson, B. Narupai, E. P. Toumayan, Y. D. Luo, A. J. McGrath, P. G. Clark, J. R. de Alaniz and C. J. Hawker, *ACS Macro Lett.*, 2016, **5**, 258–262.
21 S. B. Tan, J. Xiong, Y. F. Zhao, J. J. Liu and Z. C. Zhang, *J. Mater. Chem. C*, 2018, **6**, 4131–4139.
22 C. H. Lim, M. D. Ryan, B. G. McCarthy, J. C. Theriot, S. M. Sartor, N. H. Damrauer, C. B. Musgrave and G. M. Miyake, *J. Am. Chem. Soc.*, 2017, **139**, 348–355.
23 S. M. Sartor, Y. M. Lattke, B. G. McCarthy, G. M. Miyake and N. H. Damrauer, *J. Phys. Chem. A*, 2019, **123**, 4727–4736.
24 D. Koyama, H. J. A. Dale and A. J. Orr-Ewing, *J. Am. Chem. Soc.*, 2018, **140**, 1285–1293.
25 S. Jockusch and Y. Yagci, *Polym. Chem.*, 2016, **7**, 6039–6043.

26 R. N. Carmean, T. E. Becker, M. B. Sims and B. S. Sumerlin, *Chem*, 2017, **2**, 93–101.
27 J. T. Xu, K. Jung, A. Atme, S. Shanmugam and C. Boyer, *J. Am. Chem. Soc.*, 2014, **136**, 5508–5519.
28 H. H. Gong, Y. Gu, Y. C. Zhao, Q. Z. Quan, S. T. Han and M. Chen, *Angew. Chem.*, 2020, **59**, 919–927.
29 L. Mueller, W. Jakubowski, K. Matyjaszewski, J. Pietrasik, P. Kwiatkowski, W. Chaladaj and J. Jurczak, *Eur. Polym. J.*, 2011, **47**, 730–734.
30 V. Percec, T. Guliashvili, J. S. Ladislaw, A. Wistrand, A. Stjerndahl, M. J. Sienkowska, M. J. Monteiro and S. Sahoo, *J. Am. Chem. Soc.*, 2006, **128**, 14156–14165.
31 J. Rzayev and J. Penelle, *Angew. Chem., Int. Ed.*, 2004, **43**, 1691–1694.
32 K. Matyjaszewski, *Adv. Mater.*, 2018, **30**, 22.
33 A. J. D. Magenau, N. C. Strandwitz, A. Gennaro and K. Matyjaszewski, *Science*, 2011, **332**, 81–84.
34 S. Park, P. Chmielarz, A. Gennaro and K. Matyjaszewski, *Angew. Chem., Int. Ed.*, 2015, **54**, 2388–2392.
35 B. Li, B. Yu, W. T. S. Huck, W. M. Liu and F. Zhou, *J. Am. Chem. Soc.*, 2013, **135**, 1708–1710.
36 M. Fantin, A. A. Isse, A. Venzo, A. Gennaro and K. Matyjaszewski, *J. Am. Chem. Soc.*, 2016, **138**, 7216–7219.
37 J. R. Wang, M. Y. Tian, S. Q. Li, R. Wang, F. P. Du and Z. G. Xue, *Polym. Chem.*, 2018, **9**, 10.
38 Y. Du, R. M. Pearson, C. H. Lim, S. M. Sartor, M. D. Ryan, H. S. Yang, N. H. Damrauer and G. M. Miyake, *Chem. – Eur. J.*, 2017, **23**, 10962.
39 C. E. Dahm and D. G. Peters, *J. Electroanal. Chem.*, 1996, **402**, 91–96.
40 A. I. Popov and D. H. Geske, *J. Am. Chem. Soc.*, 1958, **80**, 1340–1352.
41 H. E. Zittel and F. J. Miller, *Anal. Chim. Acta*, 1967, **37**, 141–150.
42 T. Iwasita and M. C. Giordano, *Electrochim. Acta*, 1969, **14**, 1045–1059.
43 G. D. Allen, M. C. Buzzeo, C. Villagran, C. Hardacre and R. G. Compton, *J. Electroanal. Chem.*, 2005, **575**, 311–320.
44 M. P. S. Mousavi, S. A. Saba, E. L. Anderson, M. A. Hillmyer and P. Buhlmann, *Anal. Chem.*, 2016, **88**, 8706–8713.
45 Frit porosity and sizes, https://adamschittenden.com/technical/frits/frit-size#EuroPorosities, (accessed April 2020).
46 R. Hoffman, V. I. Minkin and B. K. Carpenter, *Int. J. Philos. Chem.*, 1997, **3**, 3–28.
47 M. D. Ryan, R. M. Pearson, T. A. French and G. M. Miyake, *Macromolecules*, 2017, **50**, 4616–4622.